

Electronic Supplementary Information

SnP nanocrystals as anode material for Na-ion battery

Junfeng Liu,^{‡a} Shutao Wang,^{‡bc} Kostiantyn Kravchyk,^{*bc} Maria Ibáñez,^{bc} Frank Krumeich,^b Roland Widmer,^d Déspina Nasiou,^e Michaela Meyns,^{*a} Jordi Llorca,^f Jordi Arbiol,^{eg} Maksym V. Kovalenko,^{bc} Andreu Cabot^{*ag}

^a Catalonia Institute for Energy Research – IREC, 08930 Sant Adrià de Besòs, Barcelona, Spain

^b Institute of Inorganic Chemistry, Department of Chemistry and Applied Biosciences, ETH Zürich, Zürich, CH-8093, Switzerland

^c EMPA-Swiss Federal Laboratories for Materials Science and Technology, Dübendorf, CH-8600, Switzerland

^d Nanotech@surface Laboratory, EMPA-Swiss Federal Laboratories for Materials Science and Technology, CH-8600, Switzerland

^e Catalan Institute of Nanoscience and Nanotechnology (ICN2), CSIC and BIST, Campus UAB, Bellaterra, 08193 Barcelona, Catalonia, Spain

^f Institute of Energy Technologies, Department of Chemical Engineering and Barcelona Research Center in Multiscale Science and Engineering. Universitat Politècnica de Catalunya, EEBE, 08019 Barcelona, Spain

^g ICREA, Pg. Lluís Companys 23, 08010 Barcelona, Catalonia, Spain

Table of Contents

1. Synthesis of tin phosphide using different tin precursors	2
2. Influence of reaction temperature	3
3. Influence of the amount and type of phosphonic acid.....	4
4. Influence of OAm	7
5. Influence of the reaction time	8
6. Additional HRTEM characterization.....	9
7. Additional XPS data.....	11
8. Additional electrochemical characterization	12
9. References.....	15

1. Synthesis of tin phosphide using different tin precursors

In a typical synthesis, 0.2 mmol of the selected tin precursor (bis[bis(trimethylsilylamino)tin(II), tin(II) stearate or tin(II) oxalate) and 10 mL of oleylamine (OAm) were added to a 50 mL three-necked flask containing a stir bar. The reaction mixture was stirred moderately and was heated to 100 °C under vacuum for 60 min to remove air, water and low-boiling point impurities. Then, the solution was placed under argon and heated to 250 °C within 15 min. Then, 0.1 mL of hexamethylphosphorous triamide (HMPT) was injected into the reaction flask and the reaction was kept at this temperature for 60 min. The flask was allowed to cool to 200 °C by removing the heating mantle and then cooled rapidly to room temperature with a water bath. The contents of the reaction mixture were transferred into centrifuge tubes, followed by centrifugation at 5000 rpm (3200 g) for 5 min. The isolated powder was re-suspended and precipitated using 1:3 (v:v) chloroform and ethanol and then centrifuged again. This entire process was repeated twice.

For tin(II) acetylacetonate as precursor, 10 mL of OAm was added to a 50 mL three-necked flask containing a stir bar. The mixture was stirred moderately and was heated to 100 °C under vacuum for 60 min. The solution was placed under argon and then 0.2 mmol of tin(II) acetylacetonate in 0.1 mL of octadecene was injected into the flask. The temperature was increased to 250 °C within 15 min and then 0.1 mL of HMPT was injected to the reaction flask. The reaction was kept at this temperature for 60 min. The flask was allowed to cool to 200 °C by removing the heating mantle and then cooled rapidly to room temperature with a water bath. The washing steps were the same as with the syntheses utilizing other tin precursors.

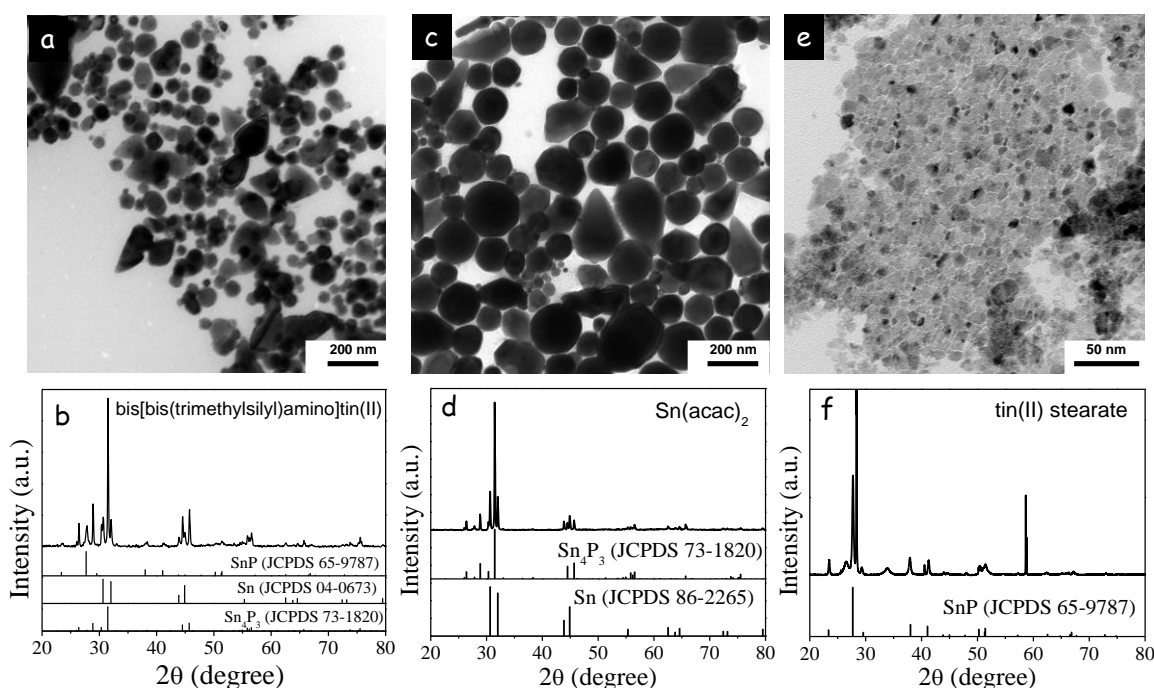


Figure S1. TEM and XRD of as-synthesized NPs by bis[bis(trimethylsilylamino)tin (a,b), tin acetylacetonate (c,d), and tin stearate (e,f) as tin precursors.

2. Influence of reaction temperature

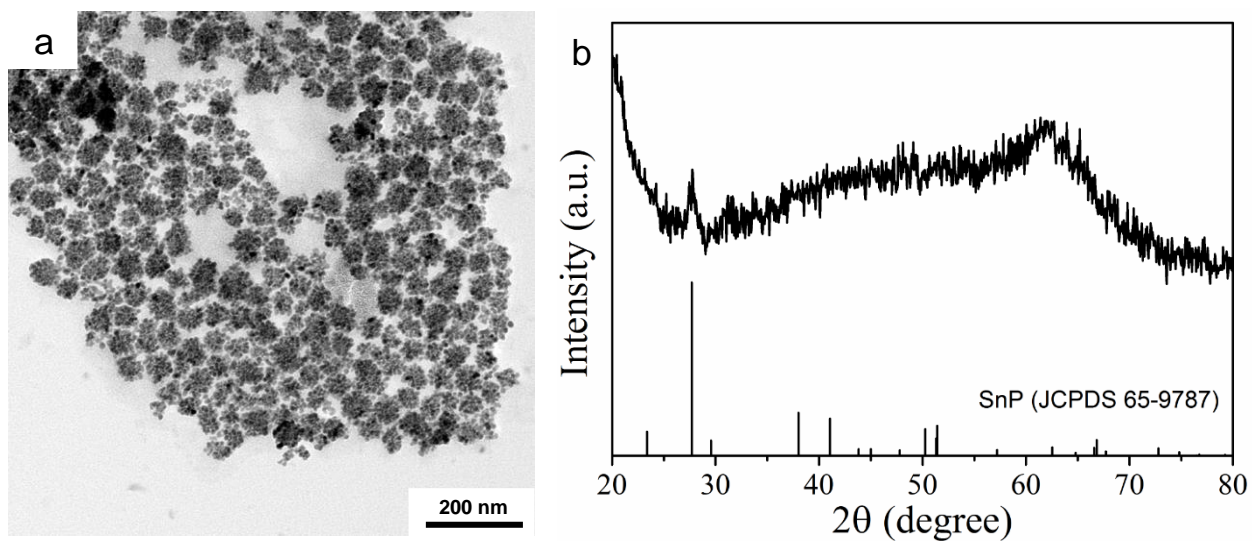


Figure S2. TEM micrograph (a) and XRD pattern (b) of SnP nanocrystals (NCs) produced at 250 °C.

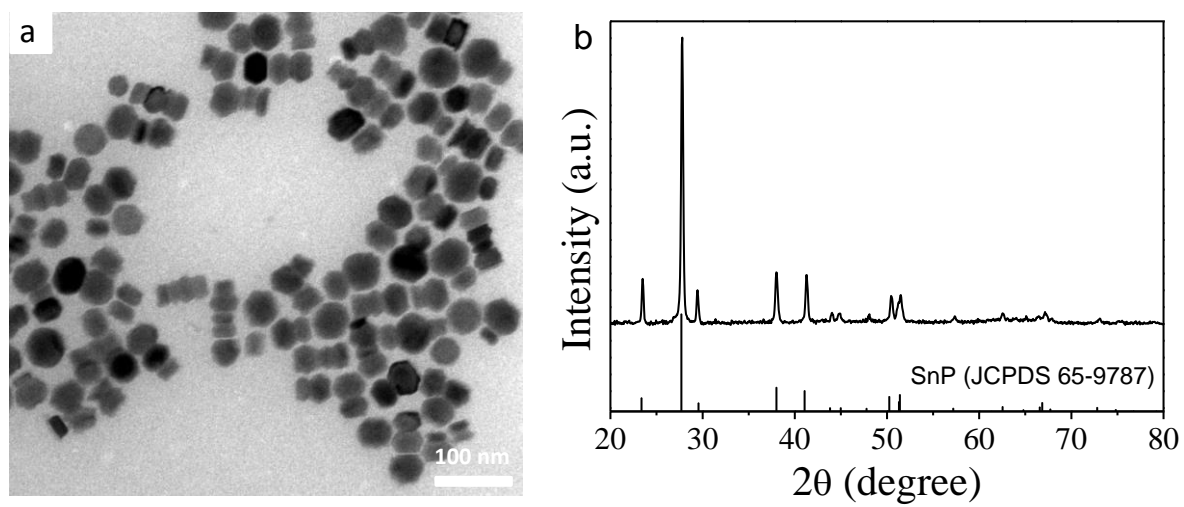


Figure S3. TEM micrograph (a) and XRD pattern (b) of SnP NCs produced at 300 °C.

3. Influence of the amount and type of phosphonic acid

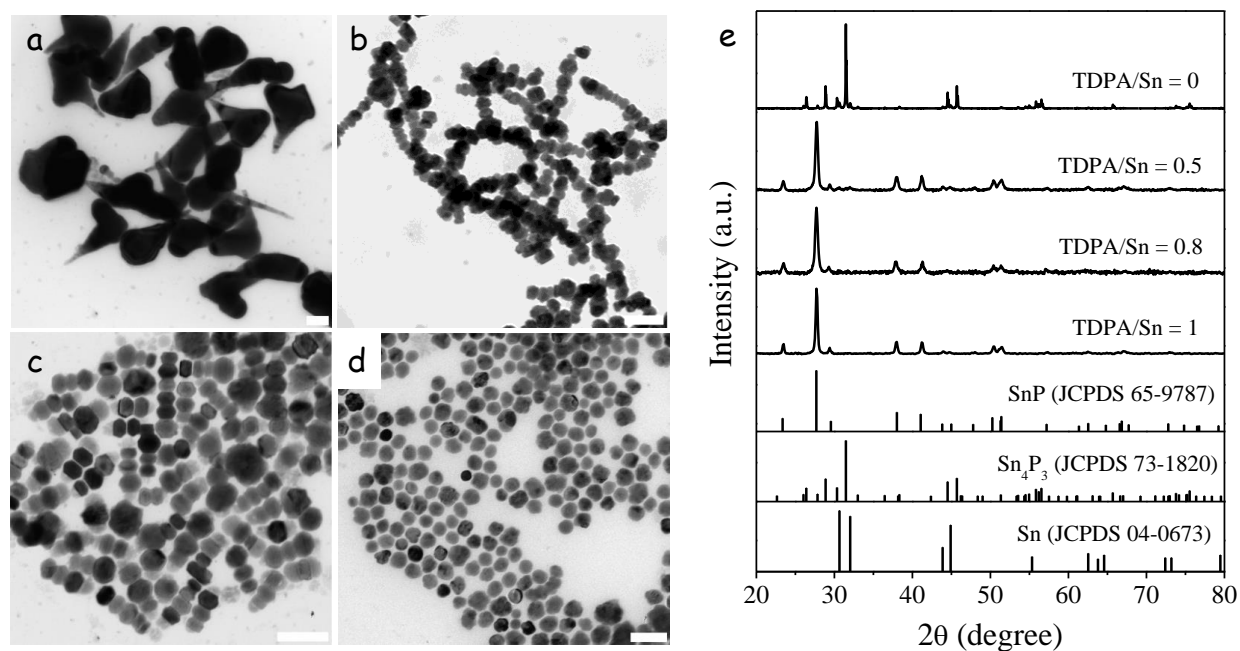


Figure S4. TEM micrographs (a-d) and XRD patterns (e) of the particles produced from the reaction of tin oxalate with HMPT at 270 °C. Reaction was carried out in octadecene and in the presence of OAm and different amounts of TDPA: a) TDPA/Sn = 0; b) TDPA/Sn = 0.5; c) TDPA/Sn = 0.8; d) TDPA/Sn = 1. Scale bars in TEM micrographs correspond to 100 nm.

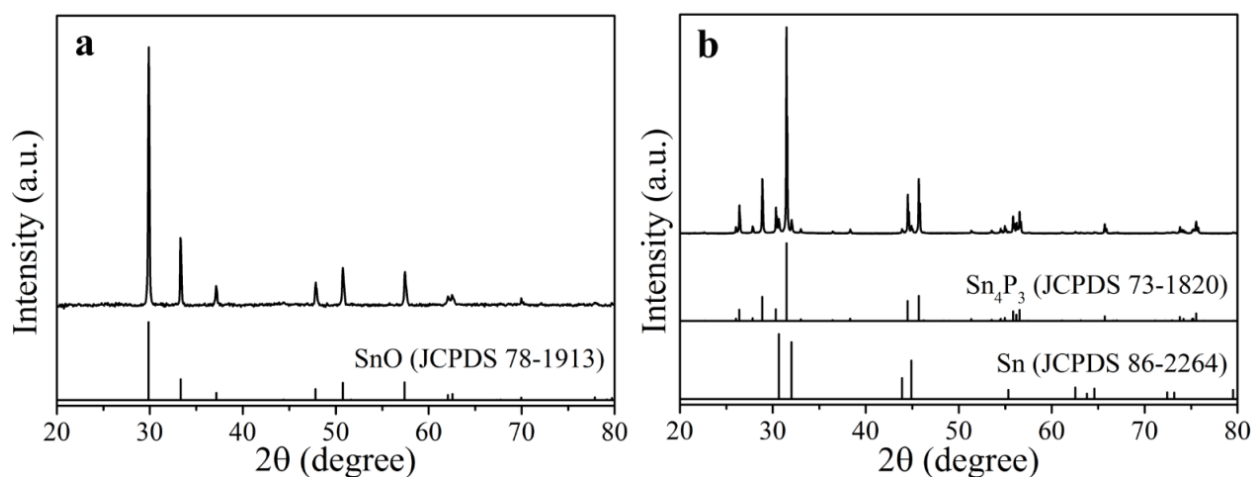


Figure S5. XRD of NCs produced without TDPA at 270 °C before injecting HMPT (a) and after reaction with HMPT for 1 h at 270 °C (b).

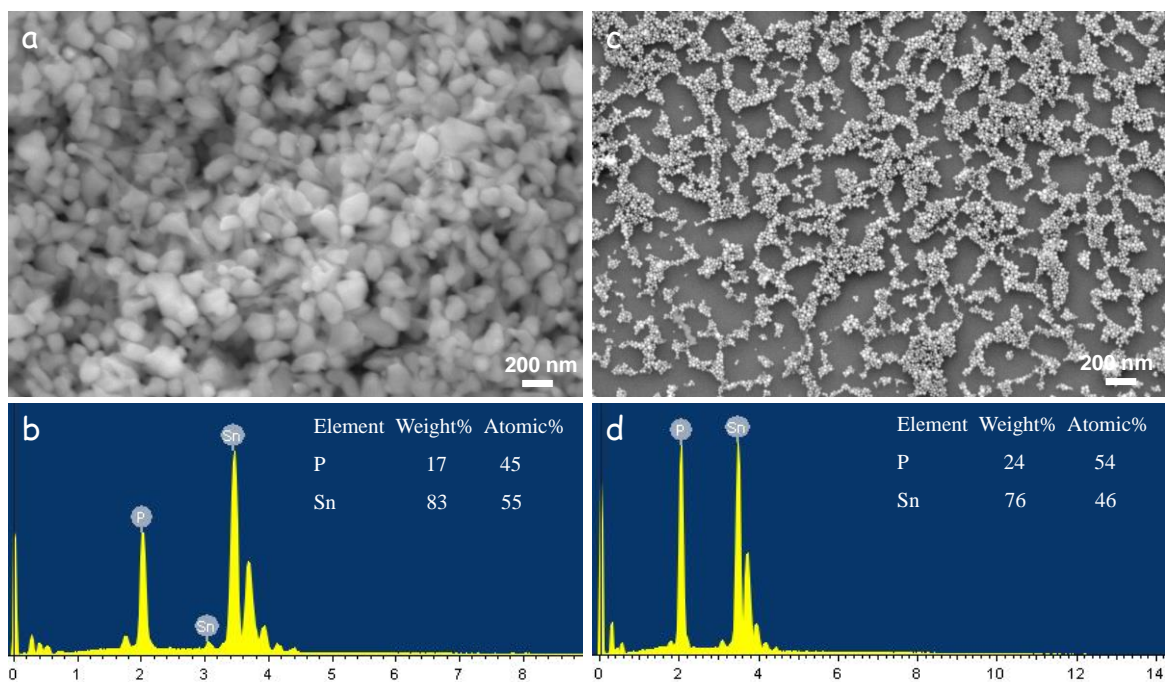


Figure S6. SEM micrograph and EDX spectrum of Sn-P NCs produced in the absence of TDPA (a, b) and in the presence of TDPA (c, d)

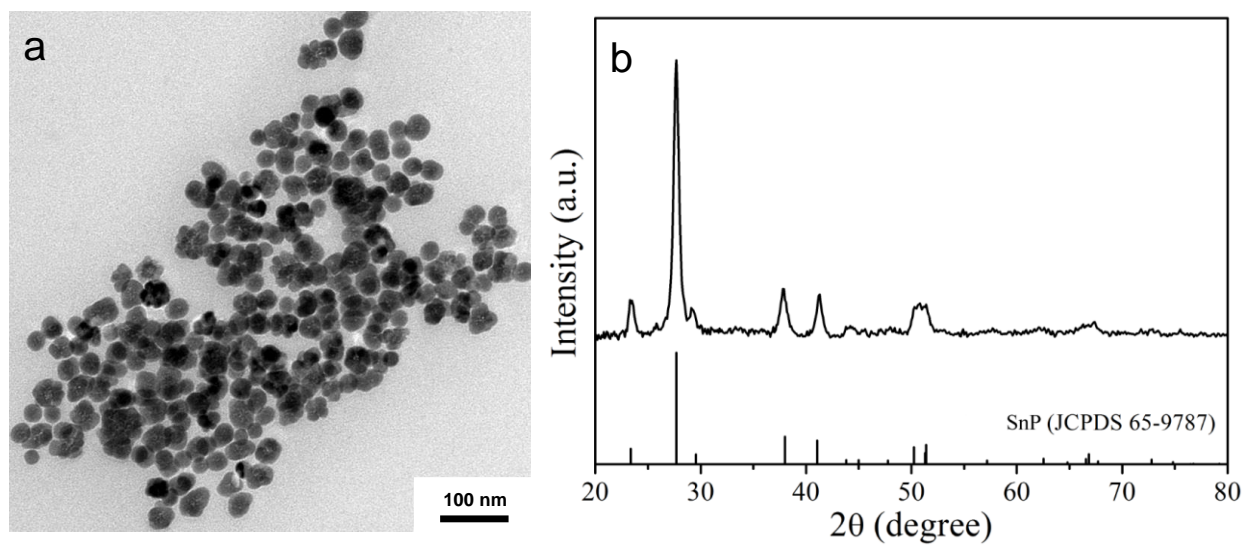


Figure S7. TEM micrograph (a) and XRD pattern (b) of SnP NCs produced with ODPA.

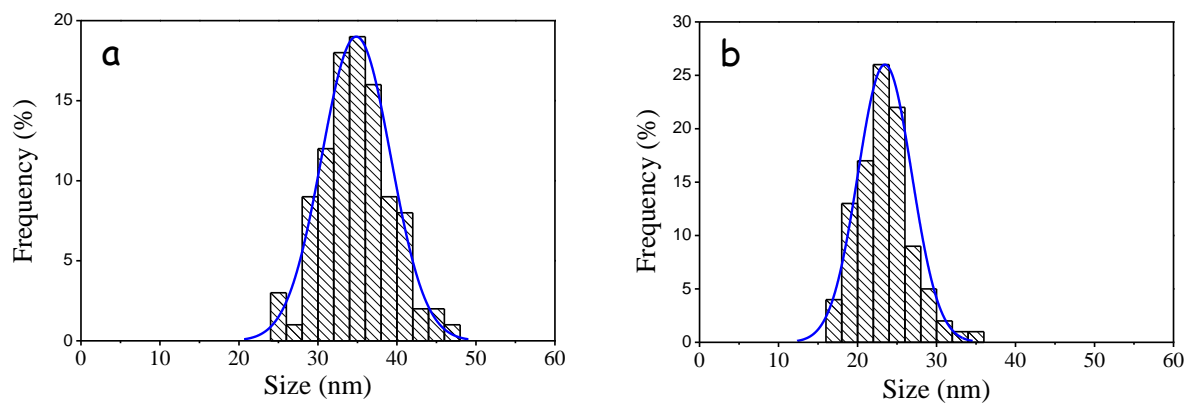


Figure S8. Size distribution of SnP synthesized utilizing TDPA (a) and ODPA (b) as ligand.

4. Influence of OAm

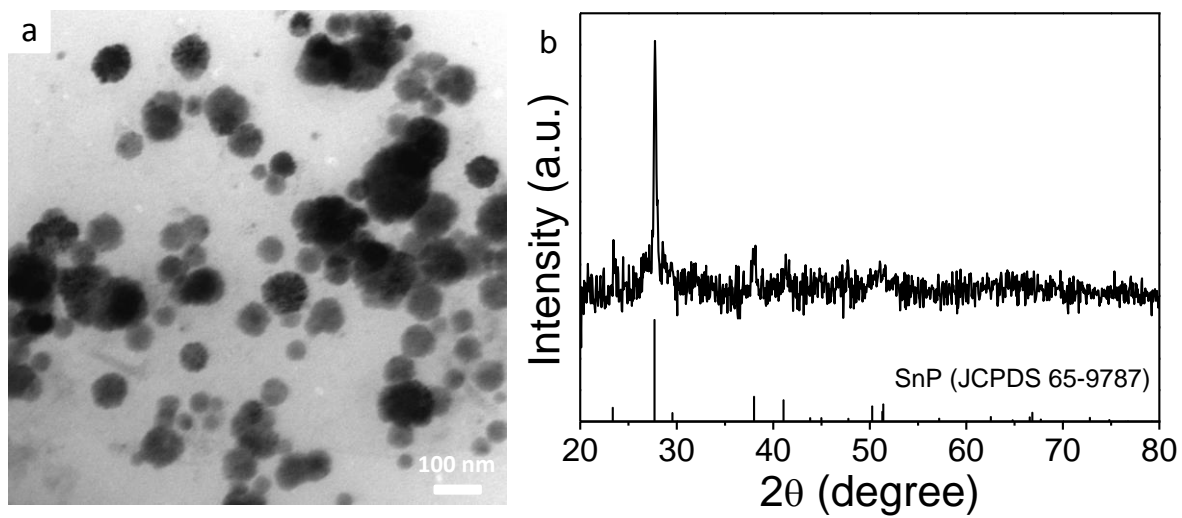


Figure S9. TEM micrograph (a) and XRD pattern (b) of SnP NCs produced without OAm.

5. Influence of the reaction time

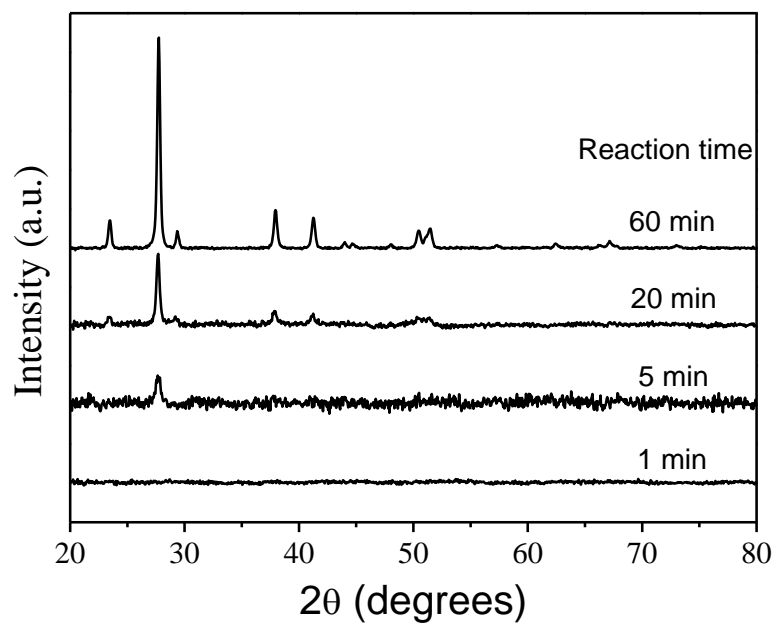


Figure S10. XRD patterns of the SnP NCs obtained after different reaction times as displayed in the graph.

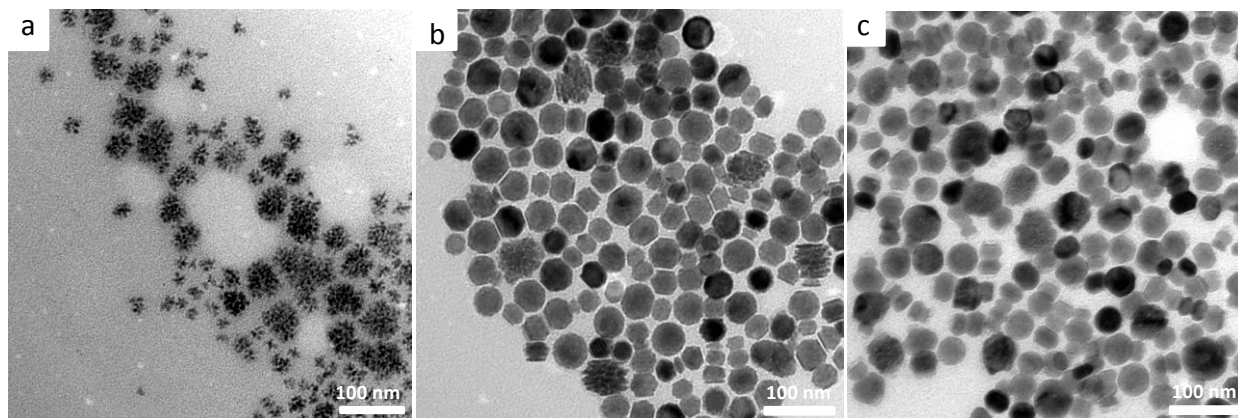


Figure S11. TEM micrographs of the SnP NCs obtained after different reaction times: a) 1 min; b) 5 min; c) 20 min. Reaction temperature was 270 °C.

6. Additional HRTEM characterization

Figure S12 shows a HRTEM micrograph taken from a SnP NC. The power spectrum (FFT) obtained from this NC reveals that it has the SnP structural phase with a trigonal symmetry (S.G.: P-3m1) and lattice parameters of $a = 4.3922 \text{ \AA}$, $b = 4.3922 \text{ \AA}$, $c = 6.0400 \text{ \AA}$, $\alpha = 90^\circ$, $\beta = 90^\circ$ and $\gamma = 120^\circ$. The NC is visualized along its [10-11] zone axis.

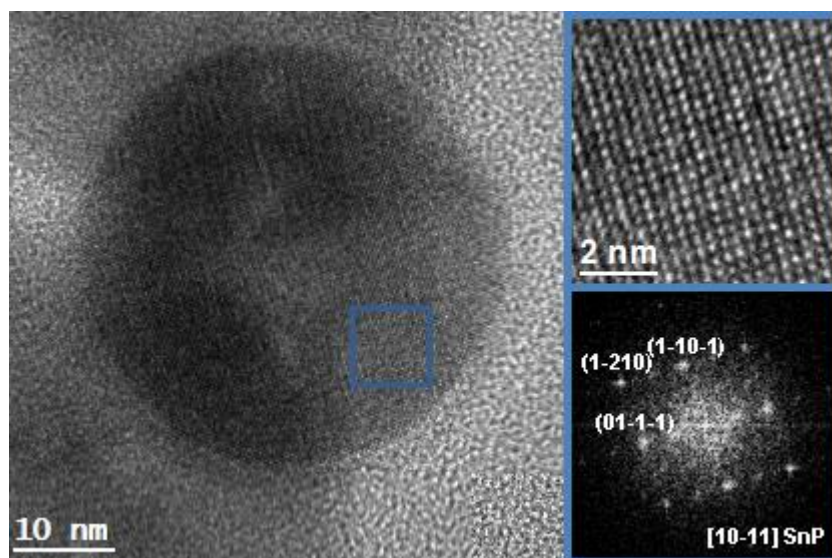


Figure S12. HRTEM micrograph of a SnP NC, (right) detail of the NC area squared in blue and its corresponding power spectrum.

Figure S13 shows a HRTEM micrograph of a SnP NC. The FFT obtained from this NC reveals that it has the SnP structural phase with a trigonal symmetry (S.G.: P-3m1) and lattice parameters of $a = 4.3922 \text{ \AA}$, $b = 4.3922 \text{ \AA}$, $c = 6.0400 \text{ \AA}$, $\alpha = 90^\circ$, $\beta = 90^\circ$ and $\gamma = 120^\circ$. The NC is visualized along its [11-23] zone axis.

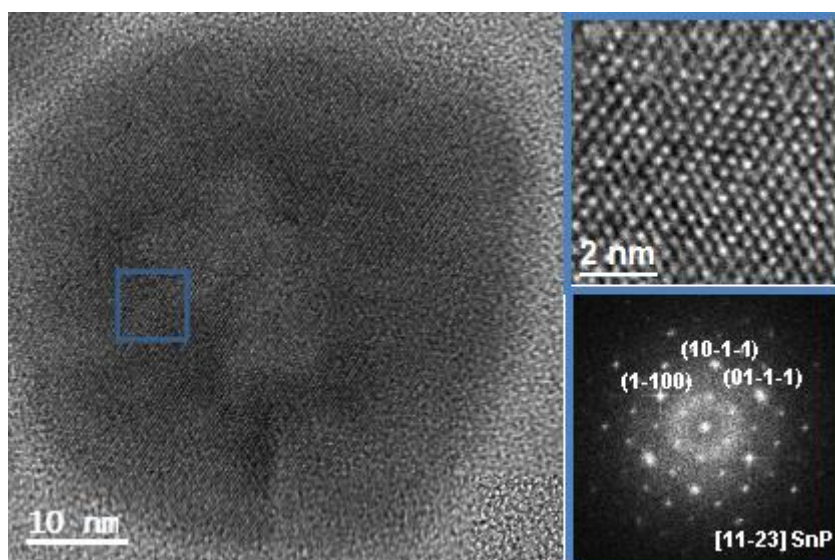


Figure S13. HRTEM micrograph of a SnP NC, (right) detail of the NC squared in blue and its corresponding power spectrum.

The presence of non-streaky extra spots in Figures S12 and S13 may indicate the presence of a certain ordered superstructure as suggested also by J.Gullman.¹ This superstructure could be related to the organized orientation of the diphosphorous pairs within the complex layers of filled octahedra. The structure model for a compound of the SnP type with the atomic pairs all oriented parallel with the c -axis was predicted by Hulliger.² Every one of these 4 pair orientations in the Sn octahedra presents an occupancy of about 25%, meaning that in the ideal material only one of the 4 diphosphorous pair orientations would be occupied. If the occupied pair orientations were randomly distributed, the expected electron diffractions and the power spectra should not present extra spots. However, when the diphosphorous pair orientations are ordered, with certain orientations preferentially fixed, then a superstructure is formed, resulting in extra spots (by following basic Bragg diffraction symmetry rules).

The observed reflections in the FFT (Figure S14) show some extra spots, circled in red, which do not exist in the ideal SnP trigonal structure with a random distribution of the P2 pairs orientations. Only the brightest spots from the FFT, circled in green, can be indexed (figure S14). A superstructure manifests itself through additional reflections every half distance.

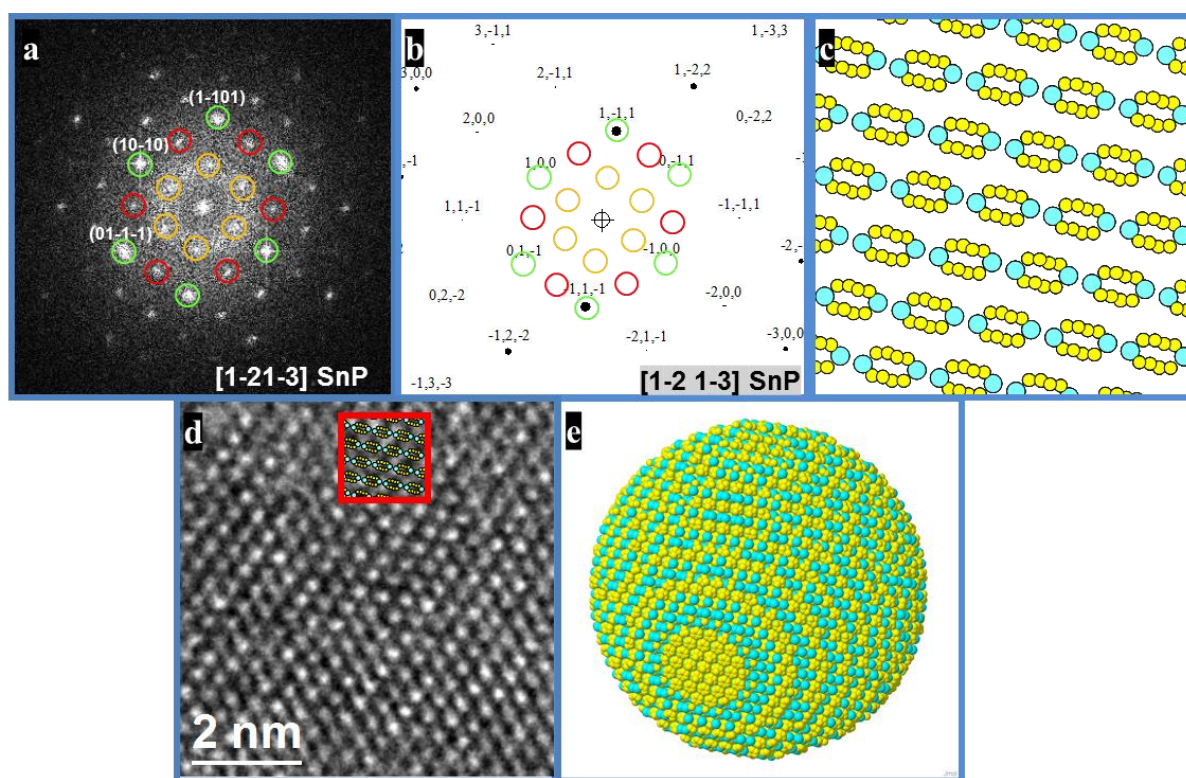


Figure S14. (a) Power spectrum (FFT) taken from the HRTEM image in Figure S13. (b) Calculated electron diffraction pattern for the equivalent $[11-23]$ zone axis in the pure SnP structure (random P2 pair orientations distribution). (c) Atomic arrangement of the Sn (cyan) and the P (yellow) atoms in the SnP structure along the $[11-23]$ zone axis. (d) HRTEM experimental detail of a SnP NC along the $[11-23]$ zone axis. (e) 3D atomic modeling of a 10 nm diameter SnP NC along the $[11-23]$ zone axis.

7. Additional XPS data

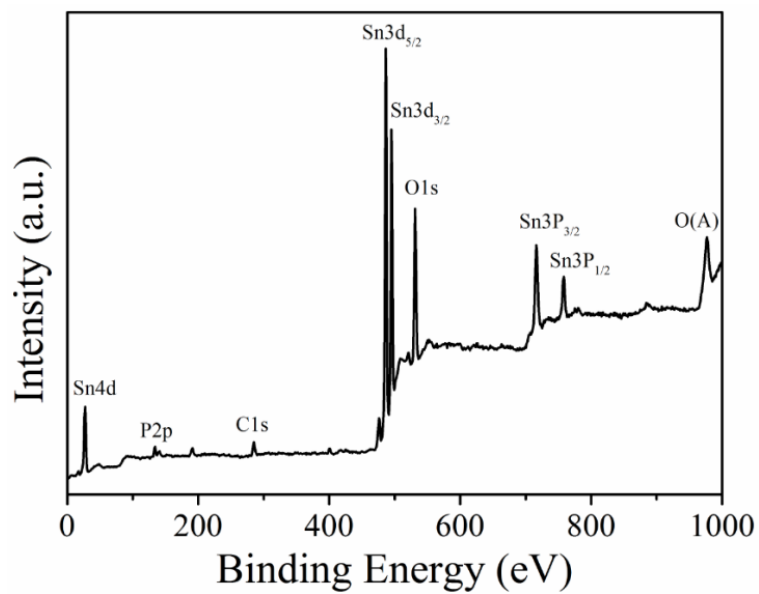


Figure S15. XPS survey of SnP.

8. Additional electrochemical characterization

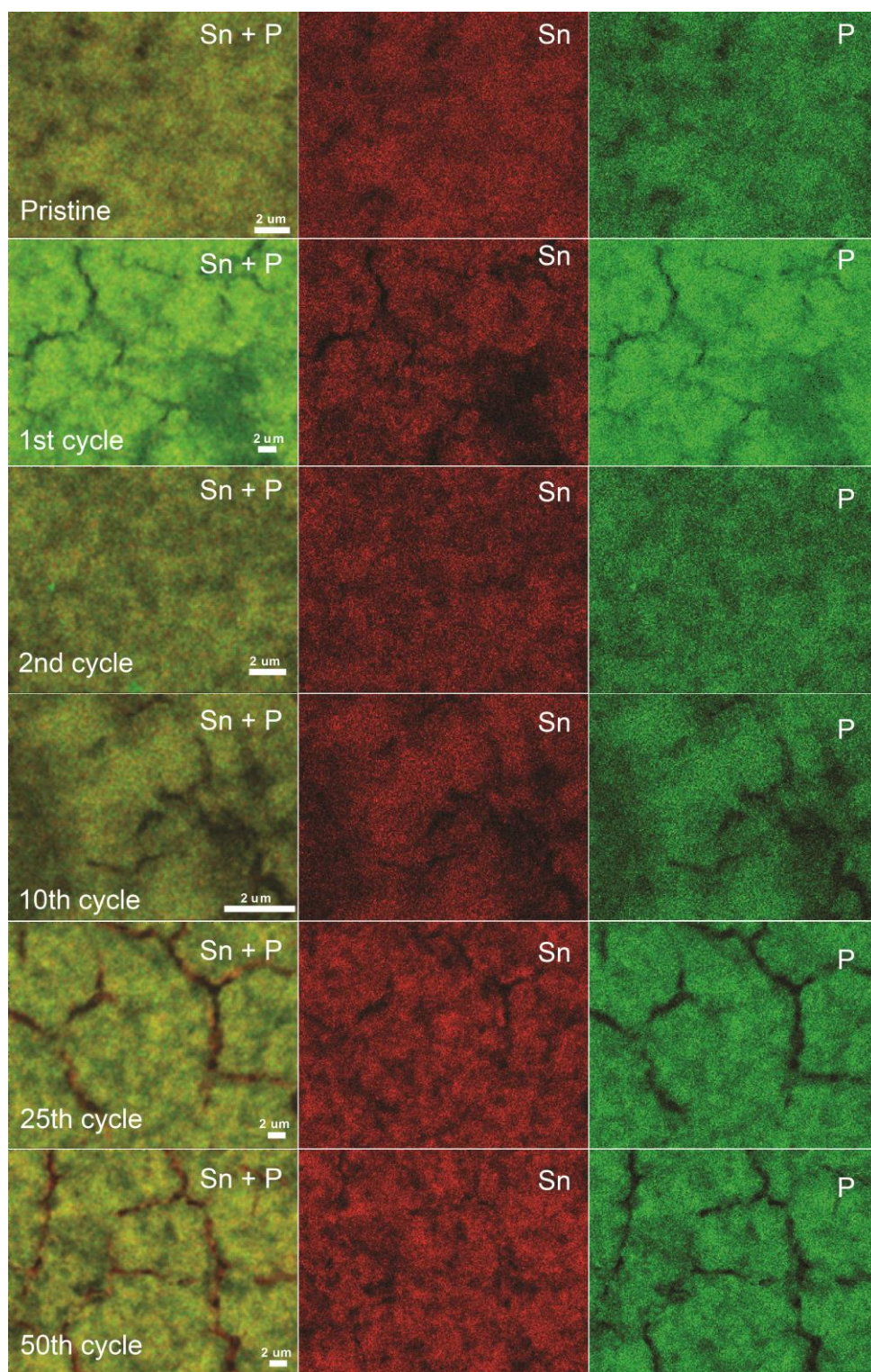


Figure S16. SEM-EDX compositional maps of electrodes comprising SnP NCs measured before (pristine) and after (1st, 2nd, 10th, 25th, 50th cycles) electrochemical cycling.

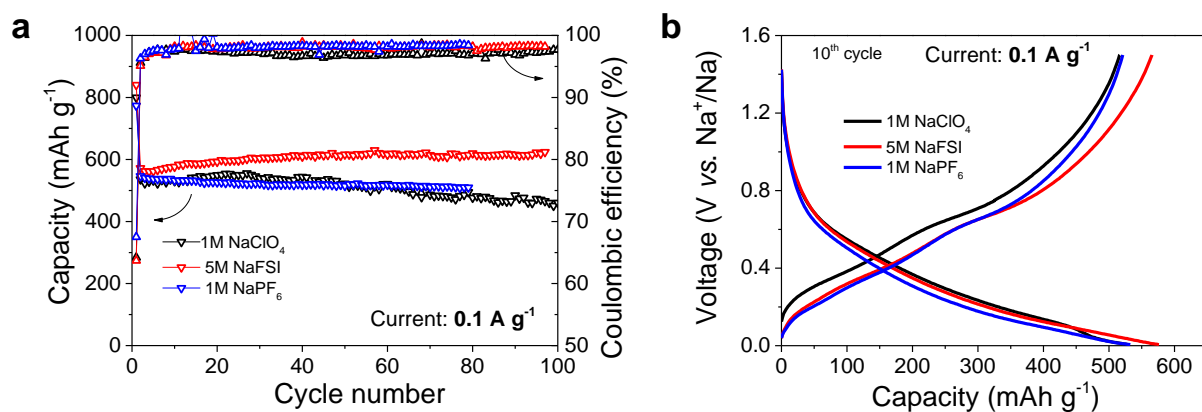


Figure S17. Cycling performance (a) and galvanostatic charge-discharge voltage curves (b) of SnP NCs measured with various sodium electrolytes. The batteries were cycled in the potential range of 5 mV-1.5 V.

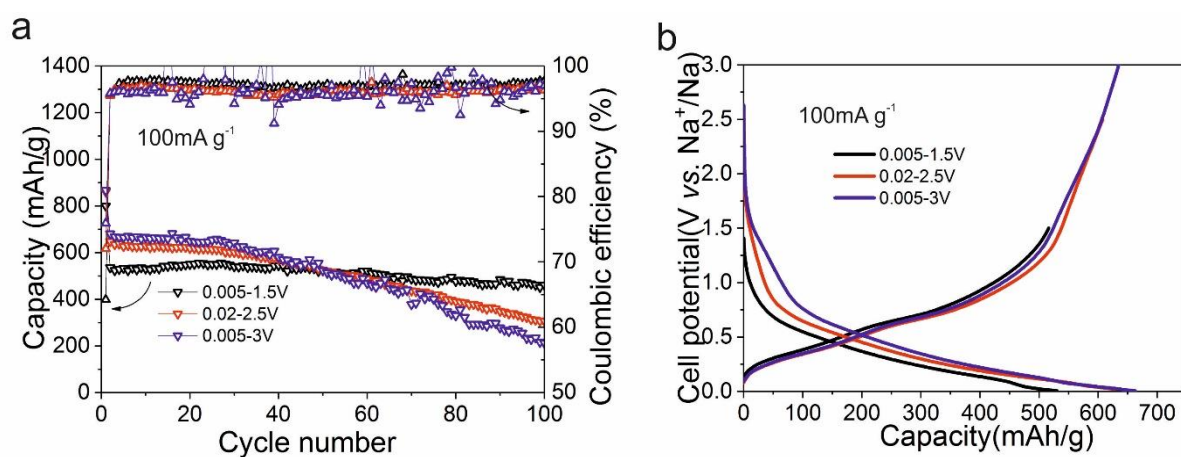


Figure S18. Cycling performance (a) and galvanostatic charge-discharge voltage curves (b) of SnP NCs at various cut off ranges. The measurements were performed in 5 M NaFSI in DME electrolyte.

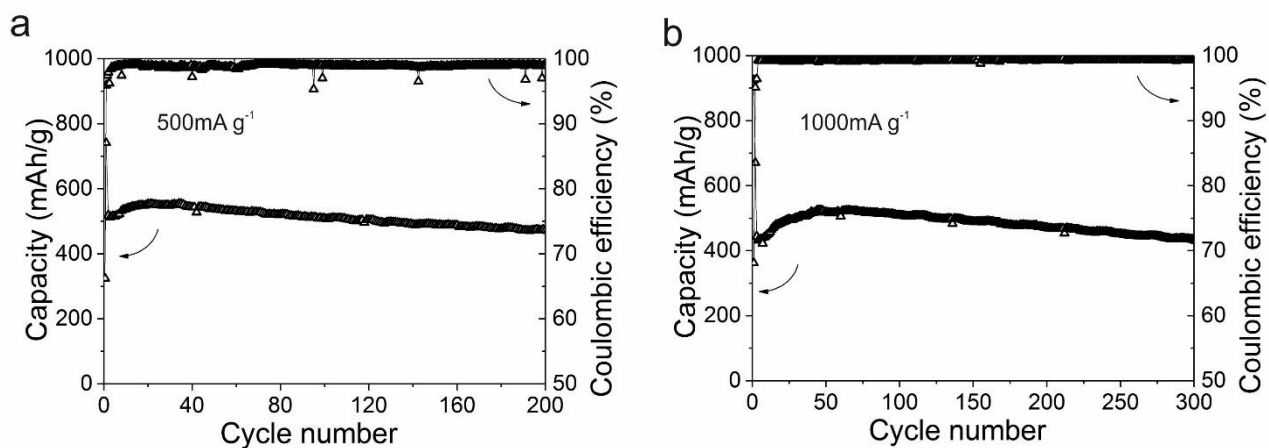


Figure S19. Cycling performance of the SnP electrode at current densities of 500 mA g⁻¹ (a) and 1000 mA g⁻¹ (b).

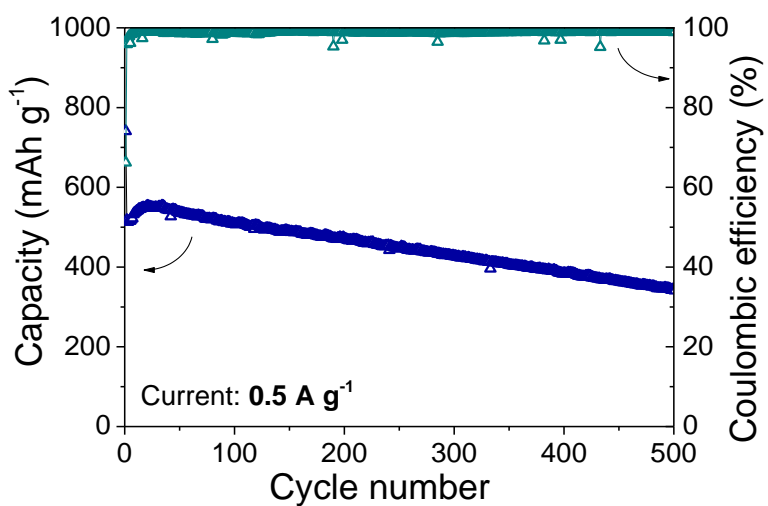


Figure S20. Cyclic stability of a Na-ion half-cell employing SnP anode made from SnP NCs at 0.5 A g⁻¹.

9. References

1. J. Gullman, *J. solid state Chem.*, 1990, **87**, 202-207.
2. F. Hulliger, *Structural Chemistry of Layer-Type Phases*. Dordrecht, Holland, 1976, pp. 145.